

# NJC

Accepted Manuscript



This is an *Accepted Manuscript*, which has been through the Royal Society of Chemistry peer review process and has been accepted for publication.

*Accepted Manuscripts* are published online shortly after acceptance, before technical editing, formatting and proof reading. Using this free service, authors can make their results available to the community, in citable form, before we publish the edited article. We will replace this *Accepted Manuscript* with the edited and formatted *Advance Article* as soon as it is available.

You can find more information about *Accepted Manuscripts* in the [Information for Authors](#).

Please note that technical editing may introduce minor changes to the text and/or graphics, which may alter content. The journal's standard [Terms & Conditions](#) and the [Ethical guidelines](#) still apply. In no event shall the Royal Society of Chemistry be held responsible for any errors or omissions in this *Accepted Manuscript* or any consequences arising from the use of any information it contains.



[www.rsc.org/njc](http://www.rsc.org/njc)

Cite this: DOI: 10.1039/c0xx00000x

www.rsc.org/xxxxxx

ARTICLE TYPE

# Surface modification of supramolecular nanotubes and selective guest capture†

Minjuan Lin,<sup>a</sup> Haoliang Liu,<sup>a</sup> Philip W. Miller,<sup>b</sup> Jianyong Zhang<sup>\*a</sup> and Cheng-Yong Su<sup>\*a</sup>

Received (in XXX, XXX) Xth XXXXXXXXX 20XX, Accepted Xth XXXXXXXXX 20XX

DOI: 10.1039/b000000x

Post modification of supramolecular assemblies via covalent capture is an important strategy for the fabrication of functional materials. This paper describes the synthesis of supramolecular nanotubes with appended pyridyl groups based on *N,N',N''*-tris(3-methylpyridyl)trimesic amide (TMPTA), and their successful post-modification by 1,4-bis(bromomethyl)benzene. The original tubular morphology of the TMPTA nanotubes was found to stay intact following the modification process. The modified nanotubes are resistant to attack by strong acids and bases. The continuous network of covalent bonds throughout the tubular network is responsible for this stability. The formation of pyridinium cations upon modification results in positively charged surfaces of nanotubes that were found to be highly effective adsorbents for a range of anionic dyes, demonstrating both high adsorption capacity and selectivities over cationic and neutral dye species. The material can be reused for dye capture without losses in their capture ability.

## Introduction

Industrial printing and fabric dyeing processes use vast amounts of water that inevitably generate waste streams of water that require treatment. The removal of these industrial dyes, many of which are harmful to aquatic life and human health, from waste water is an important process to minimise pollution.<sup>1</sup> Various adsorbents have been used to remove organic dyes from water. Silica gels and activated carbons are commonly used for such processes however these materials are mainly microporous, thus dye molecules with large size cannot easily penetrate the micropores which typically results in much lower adsorption of these dyes. To overcome this problem, mesoporous materials have been developed, including mesoporous carbon<sup>2-5</sup> and silica.<sup>6</sup> The presence of mesopores has been shown to significantly enhance the adsorption rate.<sup>7,8</sup>

Supramolecular gels are materials that are composed of relatively simple molecules that aggregate to form complex systems via non-covalent interactions such as hydrogen bonds, metal-organic coordination, hydrophobic interactions,  $\pi$ - $\pi$  interactions and van der Waals forces.<sup>9-15</sup> Recently, they have been applied for dye adsorption.<sup>16-22</sup> The three-dimensional macro-/mesoporous gel matrix generated by these materials has been found to efficiently capture dye molecules with high adsorption capacities. There are several drawbacks to these gel adsorbents. The recycling process of supramolecular gelators typically requires re-gelation following extraction with organic solvent<sup>19,20</sup> or changing pH.<sup>21,22</sup> The difficulty in recycling results from the fact that supramolecular gels are physically cross-linked,

and are generally mechanically weak, and thus susceptible to stress. This problem may be addressed by converting these thermally reversible non-covalently bonded systems into irreversible covalently cross-linked materials, thus improving their mechanical integrity. This process is known as post-modification<sup>26-28</sup> and effectively enables non-covalent supramolecular assemblies to be turned into covalent polymers.

A number of examples of mechanically robust 1D fibres via post-modification of supramolecular gels have been reported.<sup>29-35</sup> In contrast to these 1D nanofibres, nanotubular structures are occasionally observed for supramolecular gels.<sup>36-48</sup> Through gel formation, relatively uniform nanotubular materials can be fabricated in large quantities. Among the gelators, the  $C_3$  symmetrical 1,3,5-benzenetricarbonyl core was found to be a particularly versatile core unit for assembling organic nanotubes.<sup>49-51</sup> The structures are hexagonal tubular and have internal diameters typically ranging from 50 to about 500 nm. They are capable of *in situ* encapsulation of various bulky guests including dye and biomolecules,<sup>49</sup> and have shown potential applications for optoelectronic devices.<sup>51</sup>

Herein, we describe a method for the post-modification of a supramolecular gel *N,N',N''*-tris(3-methylpyridyl)trimesic amide (TMPTA) nanotubular structure via the covalent capture reaction of the available pyridyl groups with a linking alkylating agent to generate a robust and mechanically stable structure. The resulting modified nanotubular material, which has a cationic surface, was tested for the selective adsorption of a range of bulky dye molecules.

Cite this: DOI: 10.1039/c0xx00000x

www.rsc.org/xxxxxx

ARTICLE TYPE

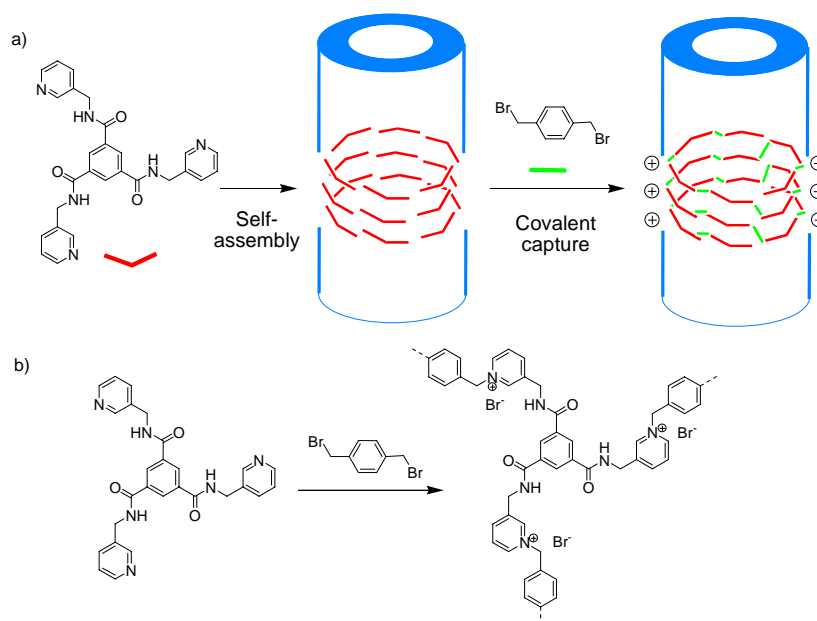


**Fig. 1** a) Schematic illustration of covalent capture of TMPTA (red units) supramolecular nanotubes via alkylation linking (green lines), and b) chemical alkylation reaction of TMPTA units with 1,4-bis(bromomethyl)benzene linker units to generate covalently bonded network.

## Results and discussion

### 5 Gelation and post-modification

*N,N',N''*-tris(3-methylpyridyl)trimesic amide (TMPTA) was chosen as the  $C_3$  symmetrical gelator because of its ability to form nanotubular structures<sup>50</sup> and its ease of synthesis. TMPTA organic nanotubes were prepared through anti-solvent-induced  
 10 instant gelation in mixed solvents recently reported by Cao *et al.*<sup>49</sup> (Fig. 1a). In a typical procedure, TMPTA (14 mg) was dissolved in ethanol (50  $\mu$ L) and mixed with an anti-solvent, toluene (200  $\mu$ L) at RT, a gel formation occurred within 1-2 min. SEM and TEM revealed that hexagonal nanotubular structures  
 15 were several microns in length and their internal diameters ranged from 200-500 nm with the wall thickness of 100-200 nm. (Fig. 2a,b). The TMPTA nanotubular structure was found to stay intact after solvent removal.

TMPTA nanotubes were post-modified via the covalent  
 20 capture reaction of 1,4-bis(bromomethyl)benzene (Fig. 1). It is widely known that pyridyl group can be alkylated with bromomethylbenzene derivatives to generate pyridinium cations. We hypothesised that 1,4-bis(bromomethyl)benzene would  
 25 bridge between two adjacent pyridyl groups on different TMPTA units to give a stable and robust polymeric product. The nanotube structure will therefore contain a continuous network of covalent bonds throughout the tubular network after modification thus giving it greater structural stability and generating charged  
 30 surfaces. The post modification of TMPTA nanotubes was achieved by simply adding a dried nanotube material to a solution of 1,4-bis(bromomethyl)benzene in MeCN and allowing to stand

for 24 hrs at RT without agitation. SEM analysis revealed that the morphology of the nanotubes was kept intact during the modification and that the modified TMPTA nanotubes have  
 35 outside diameters ranged from 500-1000 nm while the internal diameters of 200-500 nm did not change significantly from the premodified nanotubes (Fig. 2c-e). SEM also revealed that the post-modified nanotubes aggregated probably due to charge attraction and/or formation of covalent linkages between each  
 40 other, making TEM imaging of individual nanotubes more difficult.

Such modified nanotubes are effectively pyridinium type polymers, however, the tubular morphology is remarkably  
 45 different from the morphologies of other pyridinium polymers previously reported.<sup>52,53</sup> As a control experiment, direct polymerisation of TMPTA and 1,4-bis(bromomethyl)benzene in DMF yielded micrometer-sized spherical particles (Fig. 2f). The FT-IR spectrum of modified TMPTA nanotubes showed the characteristic C=N stretching vibration of the pyridyl groups at  
 50 around 1660  $\text{cm}^{-1}$  (Figure S2). The vibration is blue-shifted from that of TMPTA nanotubes at 1639  $\text{cm}^{-1}$ , attributed to the reaction of the pyridine groups with 1,4-bis(bromomethyl)benzene. PXRD of the modified nanotubes showed a weak and broad pattern (Figure S1) indicating that the long-range order present in the  
 55 original TMPTA nanotubes was lost during the post-modification. Considering the interior cavity (200-500 nm) is large enough for 1,4-bis(bromomethyl)benzene to enter, both the exterior and the interior of modified nanotubes may be modified.

Thermogravimetric analysis (TGA) demonstrated that the  
 60 modified nanotubes were thermally stable up to about 310  $^{\circ}\text{C}$

followed by decomposition (Figure S3). The weight loss evident below about 200 °C is due to the solvent release. To examine their chemical stability, the modified nanotubes were immersed in concentrated HCl or NaOH solution (pH = 12) for 2 days. SEM analysis revealed that the modified nanotubes were stable under these various acidic or basic solutions (Figure S4, S5). In contrast, the TMPTA nanotubes are readily broken by acid or base.

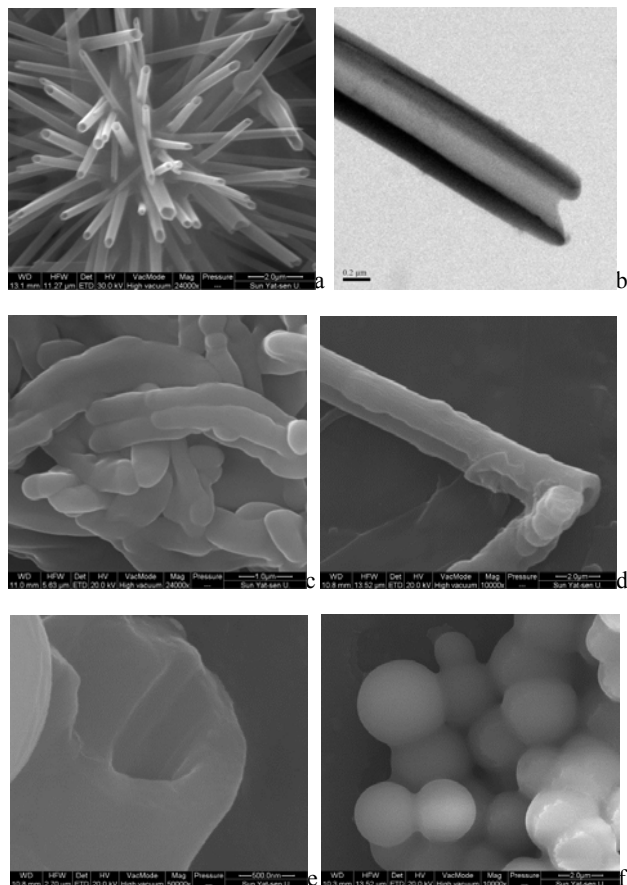


**Fig. 2** (a) SEM image of a group of TMPTA nanotubes (the white bar represents 2.0 μm), (b) TEM image of an individual TMPTA nanotube (the black bar represents 0.2 μm), and (c) SEM image of a group of modified TMPTA nanotubes (the white bar represents 1.0 μm), (d, e) SEM images highlighting individual modified TMPTA nanotubes (the white bars represent 2.0 μm and 500 nm, respectively) and (f) polymeric particles of TMPTA and 1,4-bis(bromomethyl)benzene (the white bar represents 2.0 μm).

Both modified TMPTA nanotubes and TMPTA nanotubes gave rise to similar macroporous type III isotherms indicating the overall adsorbent-adsorbate interactions are weak (Fig. S6). The N<sub>2</sub> adsorption capacity of modified TMPTA nanotubes (82.1 cm<sup>3</sup> g<sup>-1</sup>) is compared with that of TMPTA nanotubes (67.5 cm<sup>3</sup> g<sup>-1</sup>) at 1 bar. The slightly larger value is possibly attributed to the aggregation of post-modified nanotubes.

### Dye uptake experiments

To study the adsorption property of modified TMPTA nanotubes, various bulky organic molecules were selected as model guest molecules, including Rhodamine B (RB), brilliant blue R-250 (BBR-250), methyl orange (MO), Orange G (OG), Congo red (CR), methyl blue (MB) (Table 1). Among them, MO, OG, CR

and MB are anionic dyes with sulfonate groups. RB is cationic with quaternary ammonium groups and DMP is a neutral compound. BBR-250 has both anionic sulfonate and cationic quaternary ammonium groups. Dye adsorption was monitored by UV-vis spectroscopy.

Adsorption kinetics was investigated in order to understand the adsorption dynamics of modified TMPTA nanotubes. The effect of contact time on the adsorption of dye molecules is depicted in Figure 3a. A fast adsorption occurred during the first 10 min and then reached the equilibrium after 10–20 min. The adsorption capacities ( $q_e$ ) of modified TMPTA nanotubes are as the following order, OG (1290 mg g<sup>-1</sup>) > CR (1275 mg g<sup>-1</sup>) > MO (898 mg g<sup>-1</sup>) > BBR-250 (709 mg g<sup>-1</sup>) > MB (603 mg g<sup>-1</sup>) > RB (86 mg g<sup>-1</sup>) > DMP (0 mg g<sup>-1</sup>) (Table 1).

**Table 1** Structures of guest molecules used in this study and adsorption capacities of modified TMPTA nanotubes for these guest molecules.

Guest Molecule	Abbreviation	Z	$q_e$ /mg g <sup>-1</sup> ( $q_e$ /mmol g <sup>-1</sup> )
	MO	-1	898 (2.743)
	OG	-2	1290 (2.852)
	CR	-2	1275 (1.830)
	MB	-2	603 (0.754)
	BBR-250	zwitterion	709 (0.830)
	RB	+1	86 (0.180)
	DMP	0	0 (0) <sup>a</sup>

<sup>a</sup> No adsorption was observed.

The results show that the capacity of dye removal is remarkably high for all the anionic dyes with sulfonate groups (MO, OG, CG and MB). The capacity is also notable for BBR-250 with both anionic sulfonate and cationic quaternary ammonium groups. The values of the present materials are superior or comparable to those of previously reported mesoporous adsorbents (e.g., MPSC/C, 637 mg g<sup>-1</sup> for MO;<sup>2</sup> C-4@Fe, 637 mg g<sup>-1</sup> for MO;<sup>54</sup> C-1@Fe, 739 mg g<sup>-1</sup> for CR;<sup>54</sup> C-3.5, 1044 mg g<sup>-1</sup> for CR<sup>55</sup>). In contrast, cationic RB which contains quaternary ammonium groups, and DMP which is uncharged displayed negligible adsorption on modified TPMTA nanotubes.

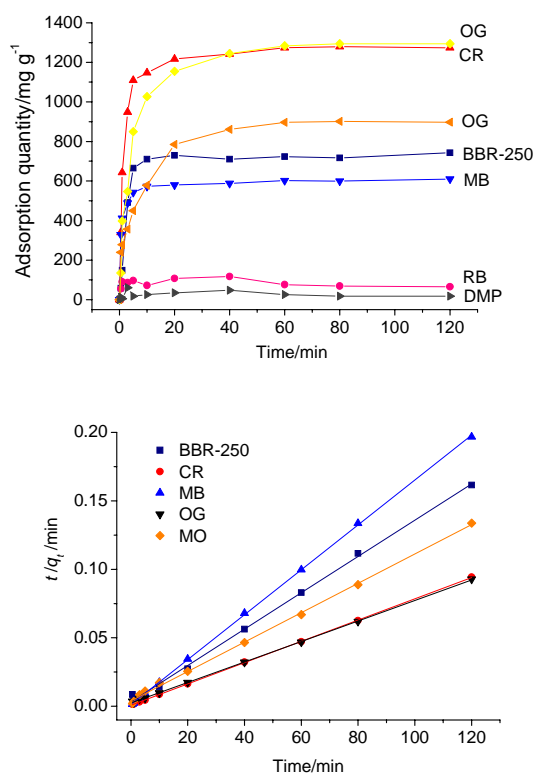


**Fig. 3** a) Effect of contact time on adsorption rate of the modified nanotubes (initial concentration of the dyes  $c = 100 \text{ mg L}^{-1}$ ), and b) pseudo-second-order kinetic plots for the dye adsorption by modified nanotubes at RT.

To reveal the relationship between the nanotube charges and guest uptake, elemental analysis was performed. The results by oxygen bomb ashing combustion and ion chromatography showed that about 3.309 mmol g<sup>-1</sup> (26.44%) of Br<sup>-</sup> was present in the modified materials, which is constant with the content of N (9.84%). For relatively small dyes MO and OG, 2.743 and 2.852 mmol g<sup>-1</sup> of dye molecules were absorbed, respectively, when the adsorption reached the equilibrium. This shows that maximum 83% or 86% of Br<sup>-</sup> ions were replaced by the dye molecules. For bulkier CR molecules ( $2.56 \times 0.78 \times 0.32 \text{ nm}^3$ ), maximum 55% of Br<sup>-</sup> ions were replaced. For the most bulky MB and BBR-250, only 0.754 and 0.830 mmol g<sup>-1</sup> of dye molecules were absorbed, respectively.

The pseudo-second-order rate equation (1) was evaluated to analyse the adsorption rate based on the experimental data.

$$\frac{t}{q_t} = \frac{1}{k_2 q_e^2} + \frac{1}{q_e} t \quad (1)$$

where  $q_t$  and  $q_e$  are the amount of the dye adsorbed at time  $t$  and at equilibrium, respectively.  $k_2$  stands for the pseudo-second-order rate constant of adsorption ( $\text{g mg}^{-1} \text{ min}^{-1}$ ). Linear plot feature of  $t/q_t$  vs  $t$  was achieved for MO, OG, CR, MB and BBR-250 (Fig. 3b). The  $k_2$  values were calculated to be  $2.30 \times 10^{-4} \sim 2.08 \times 10^{-3} \text{ g mg}^{-1} \text{ min}^{-1}$  from the slopes and the intercepts (summarized in Table S1). The correlation coefficients of the pseudo-second-order rate model for the linear plots are close to 1, suggesting that kinetic adsorption of the TPMTA nanotubes can be described by the pseudo-second-order rate equation.

The tubular morphology of the present material contributes to the high adsorption capacity as revealed by control experiments. For the adsorption of BBR-250 on the polymeric particles that are shown in Fig. 2f, the kinetic adsorption can also be described by the pseudo-second-order rate equation (Fig. 4). This is expected because both the materials are pyridinium type polymers. But interestingly the adsorption capacity ( $q_e$ ) of the modified nanotubes (709 mg g<sup>-1</sup>) was remarkably superior to that of polymeric particles (165 mg g<sup>-1</sup>). It suggests that the bulky dye molecules (e.g., BBR-250) may not only bind to the exterior of the modified nanotubes but also penetrate the nanobutes, thus showing better adsorption capabilities.

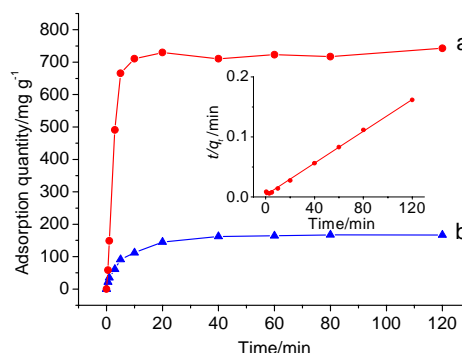


**Fig. 4** Comparison of the adsorption behaviours of BBR-250 on a) modified nanotubes and b) polymeric particles (initial concentration of the dyes  $c = 100 \text{ mg L}^{-1}$ ), with the inset showing the pseudo-second-order kinetic plot ( $R^2 = 0.99784$ ) for polymeric particles.

### Recyclability of modified TPMTA nanotubes

Regeneration and recyclability of adsorbents is a crucial aspect for their practical use. The release of the dye from the present materials was achieved by immersing in NaCl saturated solution. As a representative, the recycled materials from the BBR-250 adsorption turned visually from blue to colourless and re-captured BBR-250 dye molecules with adsorption capacity of 717 mg g<sup>-1</sup> for the second use and of 702 mg g<sup>-1</sup> for the third use at equilibrium as shown in Figure 5. The material could be recycled and used at least 5 times and the adsorption capacity did not change in the subsequent uses in comparison with the initial value of 709 mg g<sup>-1</sup>, and indicates that the modified nanotubes could be fully regenerated.

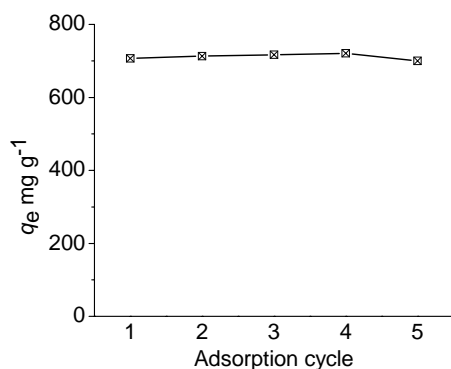


**Fig. 5** Effect of recycling on the adsorption capacity of modified nanotubes.

### Selectivity for anionic dyes by modified TMPTA nanotubes

To demonstrate the selectivity of the modified nanotubes for different dye species a solution mixture containing a cationic dye (Rhodamine B) and an anionic dye (methyl blue) was used. To a mixture of equal concentrations of MB and RB (a deep blue solution, Fig. 6) was added a quantity of modified TMPTA nanotubes. The colour of the solution gradually turned red as the MB adsorbed onto the material. The final colour of the solution was close to that of RB. During the adsorption the originally colourless nanotube powder became distinctly blue in colour, thus clearly indicating the adsorption of the anionic dye MB on the nanotubes. UV-vis spectroscopy was used to monitor this process over time and clearly showed that only the anionic guest could be trapped by the nanotubes (Fig. 7). The adsorption of MB and the other anionic dyes is clearly due to electrostatic attractive interactions between the dye anions and the pyridinium cations on the surface of the modified nanotubes. This positively charged cationic surface of the nanotubes results in high selectivity between dyes that have different charges, with the cationic RB dye showing zero uptake due to electrostatic repulsion. In comparison, no such dye selectivity was observed between cationic and anionic guests using the unmodified TMPTA nanotubular material.



**Fig. 6** Photographs showing the coloured solutions. From left to right: MB, RB, mixture of MB and RB and after addition of modified nanotubes (note the solid at the bottom of this vial which shows the blue colour of MB).

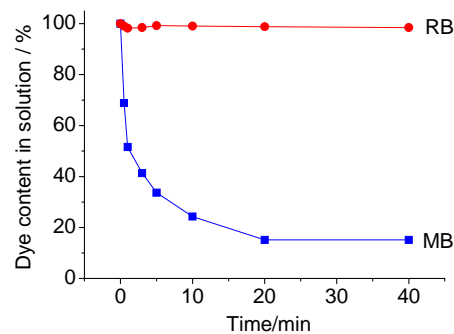
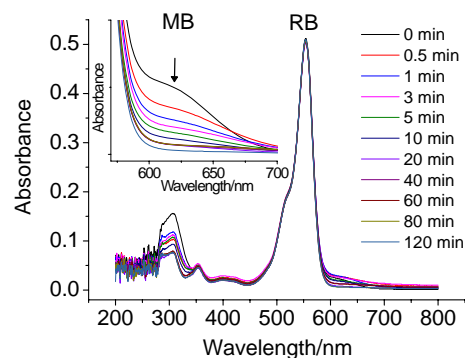


**Fig. 7** a) Time-dependent UV-vis spectra of equiconcentration RB and MB mixture in the presence of modified nanotubes, and b) percentage of RB and MB remaining in the solution monitored with time in the presence of modified nanotubes.

### Conclusions

In conclusion, stable and chemically robust *N,N,N'*-tris(3-methylpyridyl)trimesic amide (TMPTA) nanotubes with pyridinium groups can be synthesised via a covalent capture post-modification strategy using 1,4-bis(bromomethyl)benzene. The chemical stability is due to the continuous network of covalent bonds throughout the tubular network. The pyridinium cationic surface of the modified TMPTA nanotubes is responsible for the high and selective adsorption of anionic dyes over cationic or neutral species. Additionally, the modified TMPTA nanotubes could be regenerated after dye adsorption while keeping their capture capacity. In summary, post-modification of supramolecular aggregates via covalent capture is a powerful tool to generate functional materials that have greater stability and enhanced properties.

### Experimental

#### Materials and methods

Chemicals and solvents were purchased from commercial sources and used without further purification unless otherwise stated. THF was distilled over potassium under nitrogen prior to use. Scanning electron micrographs were recorded by using a JeolJSM-6330F instrument after gel samples were dispersed in hexane, put on aluminium foil and dried in vacuum. The samples were coated with a thin layer of gold prior to examination. The content of Br<sup>-</sup> was determined by oxygen bomb ashing combustion and ion chromatography. A weighed specimen was

burned in a combustion bomb containing pressed oxygen and fixed-amount of NaHCO<sub>3</sub>/Na<sub>2</sub>CO<sub>3</sub> solution. The chlorides released from the burning reaction are absorbed by NaHCO<sub>3</sub>/Na<sub>2</sub>CO<sub>3</sub> solution and determined by ion chromatography.

### Synthesis of TMPTA

TMPTA was synthesised by a modified procedure to that reported by Shi et al.<sup>50</sup> To 1,3,5-benzenetricarboxylic acid (5.00 g, 23.8 mmol) in DMF (0.2 mL) was added SOCl<sub>2</sub> (10 mL) and stirred for 1 h at RT. The reaction mixture was then brought to reflux for 5 h to give a yellowish green solution. The solution was cooled to RT and evaporated to dryness. Anhydrous THF (60 mL) was added and followed by dropwise addition of 3-aminomethyl pyridine (9.0 mL, 9.54 g, 88.3 mmol) with stirring. The reaction mixture was stirred for a further 2.5 h, and then poured into water (1 L). The resulting white precipitate was washed with water and dried under vacuum to yield a white solid (9.73 g, 85%). <sup>1</sup>H NMR (400 MHz, DMSO-*d*<sub>6</sub>) δ = 9.34 (t, *J* = 5.8 Hz, 3H), 8.58 (s, 3H), 8.50 (s, 3H), 8.47 (d, *J* = 4.1 Hz, 3H), 7.75 (d, *J* = 7.8 Hz, 3H), 7.36 (dd, *J* = 7.7, 4.8 Hz, 3H), 4.53 (d, *J* = 5.8 Hz, 6H).

### Preparation of modified TMPTA nanotubes

To a solution of TMPTA (14 mg, 0.087 mmol) in EtOH (50 μl) was added toluene (200 μl) and mixed rapidly. A white opaque gel formed within 1-2 min. The gel was dispersed in *n*-hexane to obtain a white precipitate that was filtered in air and dried under vacuum (11 mg, 79%). To a solution of 1,4-bis(bromomethyl)benzene (39.3 mg, 0.15 mmol) in MeCN (600 μL) was added the TMPTA nanotube (48 mg, several batches of the previous reaction are needed) as a solid, and allowed to stand for 1 day at RT. The white material obtained was filtered and washed with CH<sub>2</sub>Cl<sub>2</sub> and EtOH to yield the modified nanotubes (65 mg). Anal. found (calcd.) for C<sub>13</sub>H<sub>12</sub>ON<sub>2</sub>Br (*M*<sub>w</sub> = 292.16): Br 26.44 (27.35); N 9.84 (9.59)%.

### Adsorption experiments

The adsorption studies were carried out by agitating 1.0-6.0 mg of modified TMPTA nanotubes in 50 mL of dye solution. All the dyes were dissolved in deionised water (100 mg L<sup>-1</sup>). After adsorption, the dye concentration was determined using a Shimadzu UV-2450 ultraviolet-visible spectrophotometer. The wavenumbers for the maximum UV-vis absorption for MO, BBR-250, MB, RB, CR, OG, DMP were 463.5, 551.5, 595.0, 553.5, 497.5, 478.0, 284.5 nm, respectively. For the selectivity experiment of RB and MB, 3.4 mg of modified TMPTA nanotubes were agitated in a mixed solution of RB (35 mL, 100 mg L<sup>-1</sup>) and MB (35 mL, 100 mg L<sup>-1</sup>), and the wavenumbers for RB and MB were 553.5 and 610 nm, respectively.

### Acknowledgements

We acknowledge the 973 Program (2012CB821701), the NSFC (21273007 and 21350110212), the Program for New Century Excellent Talents in University (NCET-13-0615) and the Fundamental Research Funds for the Central Universities (14lgpy05) for support.

### Notes and references

- <sup>a</sup> KLGHEI of Environment and Energy Chemistry, MOE Key Laboratory of Polymeric Composite and Functional Materials, School of Chemistry and Chemical Engineering, Sun Yat-Sen University, Guangzhou, 510275, China. Tel: 86 20 8411 0539; E-mail: zhjyong@mail.sysu.edu.cn; cecssy@mail.sysu.edu.cn
- <sup>b</sup> Department of Chemistry, Imperial College London, London, SW7 2AZ, UK.
- † Electronic Supplementary Information (ESI) available: PXRD patterns, IR spectra, TG curves, SEM images, N<sub>2</sub> adsorption-desorption isotherms and parameters of the pseudo-second-order rate equation. See DOI: 10.1039/b000000x/
- 1 I. Ali, *Chem. Rev.*, 2012, **112**, 5073–5091.
  - 2 X. Zhuang, Y. Wan, C. Feng, Y. Shen and D. Zhao, *Chem. Mater.*, 2009, **21**, 706–716.
  - 3 G. Tao, L. Zhang, Z. Hua, Y. Chen, L. Guo, J. Zhang, Z. Shu, J. Gao, H. Chen, W. Wu, Z. Liu and J. Shi, *Carbon*, 2014, **66**, 547–559.
  - 4 S. Hosseini, M. A. Khan, M. R. Malekbala, W. Cheah and T. S. Y. Choong, *Chem. Eng. J.*, 2011, **171**, 1124–1131.
  - 5 Y. Dong, H. Lin, Q. Jin, L. Li, D. Wang, D. Zhou and F. Qu, *J. Mater. Chem. A*, 2013, **1**, 7391–7398.
  - 6 Y. Zhang, Z.-A. Qiao, Y. Li, Y. Liu and Q. Huo, *J. Mater. Chem.*, 2011, **21**, 17283–17289.
  - 7 S. Lei, J.-i. Miyamoto, H. Kanoh, Y. Nakahigashi and K. Kaneko, *Carbon*, 2006, **44**, 1884–1890.
  - 8 C.-T. Hsieh and H. Teng, *Carbon*, 2000, **38**, 863–869.
  - 9 N. M. Sangeetha and U. Maitra, *Chem. Soc. Rev.*, 2005, **34**, 821–836.
  - 10 J. W. Steed, *Chem. Soc. Rev.*, 2010, **39**, 3686–3699.
  - 11 M. D. Segarra-Maset, V. J. Nebot, J. F. Miravet and B. Escuder, *Chem. Soc. Rev.*, 2013, **42**, 7086–7098.
  - 12 P. Dastidar, *Chem. Soc. Rev.*, 2008, **37**, 2699–2715.
  - 13 S. S. Babu, V. K. Praveen, A. Ajayaghosh, *Chem. Rev.*, 2014, **114**, 1973–2129.
  - 14 F. Zhao, M. L. Ma and B. Xu, *Chem. Soc. Rev.*, 2009, **38**, 883–891.
  - 15 J. Zhang and C. Y. Su, *Coord. Chem. Rev.*, 2013, **257**, 1373–1408.
  - 16 D. M. Wood, B. W. Greenland, A. L. Acton, F. Rodríguez-Llansola, C. A. Murray, C. J. Cardin, J. F. Miravet, B. Escuder, I. W. Hamley, and W. Hayes, *Chem. Eur. J.*, 2012, **18**, 2692–2699.
  - 17 P. K. Sukul and S. Malik, *RSC Adv.*, 2013, **3**, 1902–1915.
  - 18 P. Chakraborty, B. Roy, P. Bairi and A. K. Nandi, *J. Mater. Chem.*, 2012, **22**, 20291–20298.
  - 19 F. Rodríguez-Llansola, B. Escuder, J. F. Miravet, D. Hermida-Merino, I. W. Hamley, C. J. Cardin and W. Hayes, *Chem. Commun.*, 2010, **46**, 7960–7962.
  - 20 X. Dou, P. Li, D. Zhang and C.-L. Feng, *Soft Matter*, 2012, **8**, 3231–3238.
  - 21 B. O. Okesola and D. K. Smith, *Chem. Commun.*, 2013, **49**, 11164–11166.
  - 22 B. Adhikari, G. Palui and A. Banerjee, *Soft Matter*, 2009, **5**, 3452–3460.
  - 23 S. Debnath, A. Shome, S. Dutta and P. K. Das, *Chem. Eur. J.*, 2008, **14**, 6870–6881.
  - 24 S. Xiang, L. Li, J. Zhang, X. Tan, H. Cui, J. Shi, Y. Hu, L. Chen, C.-Y. Su and S. L. James, *J. Mater. Chem.*, 2012, **22**, 1862–1867.
  - 25 L. Li, S. Xiang, S. Cao, J. Zhang, G. Ouyang, L. Chen and C.-Y. Su, *Nat. Commun.*, 2013, **4**, 1774.
  - 26 K. Sada, M. Takeuchi, N. Fujita, M. Numata and S. Shinkai, *Chem. Soc. Rev.*, 2007, **2**, 415–435.
  - 27 L. J. Prins and P. Scrimin, *Angew. Chem. Int. Ed.*, 2009, **48**, 2288–2306.
  - 28 B. Gong, in *Supramolecular chemistry: from molecules to nanomaterials*, Vol 7: Soft Matter, pp 1–9, John Wiley & Sons, Ltd, 2012.
  - 29 M. George and R. G. Weiss, *Chem. Mater.*, 2003, **15**, 2879–2888.
  - 30 C. S. Love, V. Chechik, D. K. Smith, I. Ashworth and C. Brennan, *Chem. Commun.*, 2005, 5647–5649.
  - 31 J. R. Moffat, I. A. Coates, F. J. Leng, and D. K. Smith, *Langmuir*, 2009, **25**, 8786–8793.
  - 32 I. A. Coates and D. K. Smith, *Chem. Eur. J.*, 2009, **15**, 6340–6344.
  - 33 J. F. Miravet and B. Escuder, *Org. Lett.*, 2005, **7**, 4791–4794.
  - 34 D. D. Diaz, K. Rajagopal, E. Strable, J. Schneider, and M. G. Finn, *J. Am. Chem. Soc.*, 2006, **128**, 6056–6057.

- 35 D. D. Díaz, J. J. Cid, P. Vázquez and T. Torres, *Chem. Eur. J.*, 2008, **14**, 9261–9273.
- 36 N. Kameta, H. Minamikawa and M. Masuda, *Soft Matter*, 2011, **7**, 4539–4561.
- 5 37 D. Pasini and M. Ricci, *Curr. Org. Synth.*, 2007, **4**, 59–80.
- 38 N. Kameta, A. Tanaka, H. Akiyama, H. Minamikawa, M. Masuda and T. Shimizu, *Chem. Eur. J.*, 2011, **17**, 5251–5255.
- 39 J. P. Hill, W. S. Jin, A. Kosaka, T. Fukushima, H. Ichihara, T. Shimomura, K. Ito, T. Hashizume, N. Ishii and T. Aida, *Science*, 2004, **304**, 1481–1483.
- 10 40 Q. Jin, L. Zhang, H. Cao, T. Wang, X. Zhu, J. Jiang and M. Liu, *Langmuir*, 2011, **27**, 13847–13853.
- 41 X. Wang, P. Duan and M. Liu, *Chem Asain J.*, 2014, **9**, 770–778.
- 42 S. Rondeau-Gagné, J. R. Néabo, M. Desroches, I. Levesque, M. Daigle, K. Cantin and J.-F. Morin, *Chem. Commun.*, 2013, **49**, 9546–9548.
- 15 43 J. Nagasawa, M. Yoshida and N. Tamaoki, *Eur. J. Org. Chem.*, 2011, 2247–2255.
- 44 L. S. Shimizu, S. R. Salpage and A. A. Korous, *Acc. Chem. Res.*, 2014, DOI: 10.1021/ar500106f.
- 20 45 L. S. Shimizu, A. D. Hughes, M. D. Smith, M. J. Davis, B. P. Zhang, H.-C. zur Loye and K. D. Shimizu, *J. Am. Chem. Soc.*, 2003, **125**, 14972–14973.
- 46 L. S. Shimizu, M. D. Smith, A. D. Hughes and K. D. Shimizu, *Chem. Commun.*, 2001, 1592–1593.
- 25 47 M. Kogiso, M. Aoyagi, M. Asakawa and T. Shimizu, *Soft Matter*, 2010, **6**, 4528–4535.
- 48 X. Gao and H. Matsui, *Adv. Mater.*, 2005, **17**, 2037–2050.
- 49 H. Cao, P. Duan, X. Zhu, J. Jiang and M. Liu, *Chem. Eur. J.*, 2012, **18**, 5546–55.
- 30 50 N. E. Shi, G. Yin, H. B. Li, M. Han and Z. Xu, *New J. Chem.*, 2008, **32**, 2011–2015.
- 51 X. Mu, W. Song, Y. Zhang, K. Ye, H. Zhang and Y. Wang, *Adv. Mater.*, 2010, **22**, 4905–4909.
- 35 52 G. Li, J. Shen and Y. Zhu, *J. Appl. Poly. Sci.*, 2000, **78**, 668–675.
- 53 G. Li and J. Shen, *J. Appl. Poly. Sci.*, 2000, **78**, 676–684.
- 54 Y. Dong, H. Lin and F. Ou, *Chem. Eng. J.*, 2012, **193-194**, 169–177.
- 55 Y. Dong, H. Lin, Q. Jin, L. Li, D. Wang, D. Zhou, F. Ou, *J. Mater. Chem. A*, 2013, **1**, 7391–7398.
- 40